3_{10} helices in channels and other membrane proteins

Ricardo Simão Vieira-Pires and João Henrique Morais-Cabral

Instituto de Biologia Molecular e Celular, Universidade do Porto, 4150-180 Porto, Portugal

Structures of three potassium channels of the six-transmembrane (TM) helix type, a ligand-gated channel, and two voltage-gated channels were solved recently by x-ray crystallography (Long et al., 2005a,b, 2007; Clayton et al., 2008). In all three channel structures, the fourth TM segment (the voltage sensor in the voltage-gated channels) of each subunit adopts a 3_{10}-helical conformation over an unusually large stretch of residues (7–11 residues). There are still many aspects of the voltage-sensing mechanism that are not understood (Tombola et al., 2006; Swartz, 2008); however, the presence of a 3_{10} conformation in the voltage sensor could provide a simple unifying explanation for many aspects of voltage sensing. Here, we present some of the properties of 3_{10} helices and discuss these properties within the structural and functional context of potassium channels and of membrane proteins.

3_{10} versus α helices

The fundamental difference between a 3_{10} helix and an α helix is how the backbone hydrogen-bonding network of the two helices is established (Fig. 1). In α helices, the carbonyl group of residue *i* interacts with the nitrogen from the amide group in residue *i*+4. Canonical α helices have the following characteristics: 3.6 residues per turn, so that consecutive residues make an angle of 100° around the helical axis, a helical rise per residue of 1.5 Å, and a helical pitch of 5.4 Å. In contrast, in 3_{10} helices the carbonyl group in residue *i* and the nitrogen of the amide group in residue *i*+3 are hydrogen bonded. Canonical 3_{10} helices have three residues per turn, with an angle of 120° between consecutive residues, a helical rise per residue of 1.93–2.0 Å, and a helical pitch of 5.8–6 Å. In very simple terms, a 3_{10} helix is more tightly wound, longer, and thinner than an α helix with the same number of residues.

Because of their potential functional impact, it is worthwhile focusing our attention on two characteristics of 3_{10} helices, stability and dynamics. There is a generalized belief among structural biologists that 3_{10} helices are inherently unstable and are, therefore, relatively rare and short, not spanning more than three to four residues. This idea has its origins in the classical studies of the helical conformation of polypeptides. When Pauling, Corey, and Branson proposed the α-helical and the 3_{10}-helical conformations as protein structural motifs, they concluded that the 3_{10} helix had a distorted hydrogen bond network and was most likely unstable (Pauling et al., 1951). Later, in a comparative study of protein structures, Barlow and Thornton (1988) analyzed 57 protein structures and showed that 32% of the total number of residues were involved in the formation of α helices; α helices presented a mean length of 10 residues, with the longest extending over 27 residues. In contrast, they found that the 3_{10} conformation was present in only 3.4% of the total number of residues; 3_{10} helices had a mean length of 3.3 residues, with just one helix spanning six residues. The authors also concluded that 3_{10} helices in proteins differed from the canonical conformation by having an average of 3.2 residues per turn instead of three residues, and noticed that 3_{10} helices are in general irregular, presenting a wide variability in their main-chain torsion angle distribution.

The very large number of protein structures currently available has revealed that long 3_{10} helices are present in proteins. A 1999 survey found 132 cases of 3_{10} helices with six amino acids or more (Pal and Basu, 1999). More recently, a structural analysis of 689 protein chains with low sequence identity (≤20%) and solved at better than 1.6-Å resolution found 1,774 3_{10} helices spanning five residues or more (Enkhbayar et al., 2006). As expected, the large majority was composed of helices with fewer than two helical turns, but a significant number spanned more than seven residues: 53 helices were 8 residues long, 13 helices were 9 residues long, 4 helices spanned 10 residues, and 1 helix was 11 residues long. This study also classified individual 3_{10} helices as regular or irregular, according to the level of variation of stereochemical parameters along the helix, and found that the percentage of irregular helices increased rapidly with length. Interestingly, the authors concluded that 3_{10} helices are para-helices, helices where long-range order is not maintained.

Clearly, the stability of a helix in a protein structure is very dependent on the packing interactions established with other protein regions. For α helix packing in

Correspondence to João Henrique Morais-Cabral: jcabral@ibmc.up.pt

Abbreviation used in this paper: TM, transmembrane.

The Rockefeller University Press $30.00
J. Gen. Physiol. Vol. 136 No. 6 585–592
www.jgp.org/cgi/doi/10.1085/jgp.201010508

proteins, it has been shown that there is a maximization of the interaction surface between helices (Bowie, 1997). In an α helix, the 3.6 residues per turn positions side chains every 100° around the helical axis, staggering the side chains and offering an extensive set of modes of interaction (Fig. 1). This arrangement therefore imposes few structural restrictions on the interacting partners and increases the probability of the stabilization of long α helices in a protein. In contrast, as a result of the ∼3.2 residues per helical turn in 3_{10} helices, side chains are disposed in a more restrictive fashion; they form ridges along the helix (Fig. 1). Intuitively, this disposition imposes specific structural requirements for the packing of long 3_{10} helices with other protein regions. In an effort to verify this idea, we performed a visual inspection of long 3_{10} helices containing at least two turns (seven or more residues) in protein structures listed in three different papers (Peters et al., 1996; Pal and Basu, 1999; Enkhbayar et al., 2006). These reports only name a small fraction of the structures included in their studies. As a result, the final pool contained 12 proteins for a total of 13 helices (Protein Data Bank accession nos. and residues in helices are listed in the legend of Fig. 2). We found two modes of packing. Mode A was observed in eight cases. In this mode, a side-chain ridge lies in a groove formed by other regions of the protein (example in Fig. 2 A). Mode B was present in four helices. In this arrangement, one or two side chains from another region of the protein pack against the 3_{10} helix face formed between the side-chain ridges (example in Fig. 2 B). A single case was observed where the helix is completely encased by the rest of the protein; this helix has a very specific sequence with four glycines and one proline out of eight residues. More quantitatively, the different modes are distinguishable by the fraction of solvent-exposed surface area, such that helices lying in a groove (mode A) tend to be less solvent exposed than in the other packing arrangement (mode B; Fig. 2 C). Overall, this simple analysis supports the idea that packing of long 3_{10} helices has specific requirements. It also highlights the need for more extensive studies of the structural context in which 3_{10} helices are found. We suggest that long 3_{10} helices are rarely observed in protein structures, not just because they might be intrinsically less stable than α helices but also because they have packing requirements that are rarely met over long extensions, resulting in the unraveling of the 3_{10} conformation or in the variability of the helical stereochemical parameters detected in many studies.

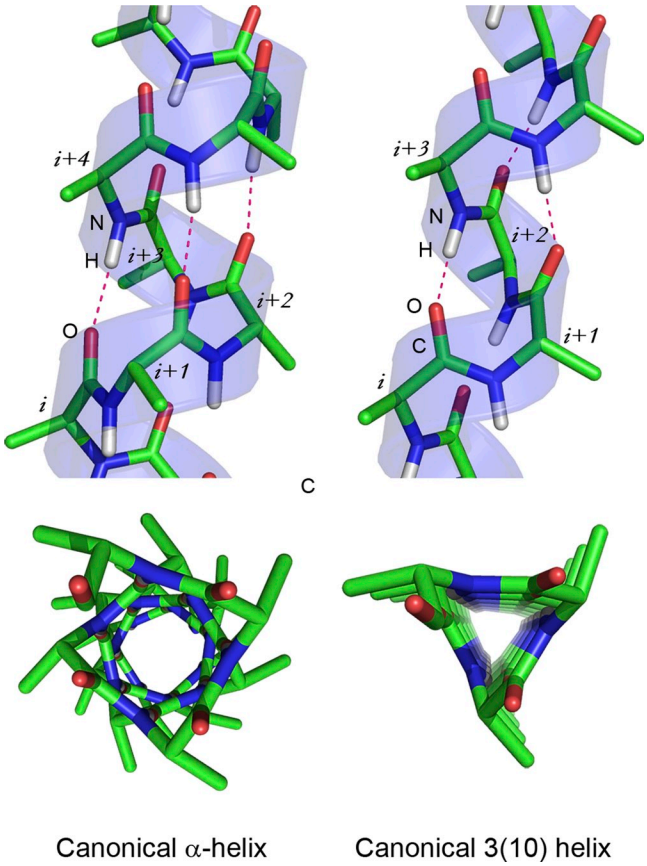

Figure 1. Canonical helical conformations. Side views and views along the axes of a helix in a canonical α-helical conformation (left) and canonical 3_{10} conformation (right). Dotted lines indicate hydrogen bonds between atoms in the backbone of polypeptide. Helices were generated using PepBuild. All figures were prepared with PYMOL.

Another important characteristic of 3_{10} helices is dynamics. This property has been well documented in isolated peptides, which are important model systems for the study of helices. In the case of 3_{10} helices, one of the best-studied systems involves peptides rich in α methylalanine, a non-natural amino acid with an extra methyl group on the α carbon (Karle and Balaram, 1990; Karle et al., 1994; Crisma et al., 2006; Bellanda et al., 2007). Because of the stereochemical constraints imposed by the presence of two large substituents in the Cα of the amino acid, these peptides have a strong tendency to adopt a helical conformation, 3_{10} or α helical. In these systems, it has been demonstrated that a peptide can adopt both conformations and that it is possible to shift the equilibrium between one conformation and the other by altering the polarity of the solvent or temperature. In some cases, these two conformations appear to coexist in the same peptide so that one region adopts a 3_{10}-helical conformation and another region adopts an α-helical conformation. A few similar observations have been documented for peptides formed by natural amino acids; the two conformations appear to be present in different segments of the peptide, and this distribution is altered by small sequence changes (Fiori et al., 1994; Dike and Cowsik, 2006; Mikhonin and Asher, 2006). Molecular dynamics studies of helices in peptides have also proposed that 3_{10} and α helices coexist along the same peptide and that interconversion between the two

conformations occurs rapidly in the nanosecond timescale (Tirado-Rives and Jorgensen, 1991; Chipot and Pohorille, 1998; Raman et al., 2008). Interestingly, the presence of main-chain bifurcated hydrogen bonds, where residue *i* is simultaneously hydrogen bonded to *i*+3 and *i*+4, has been detected by molecular dynamics (Armen et al., 2003).

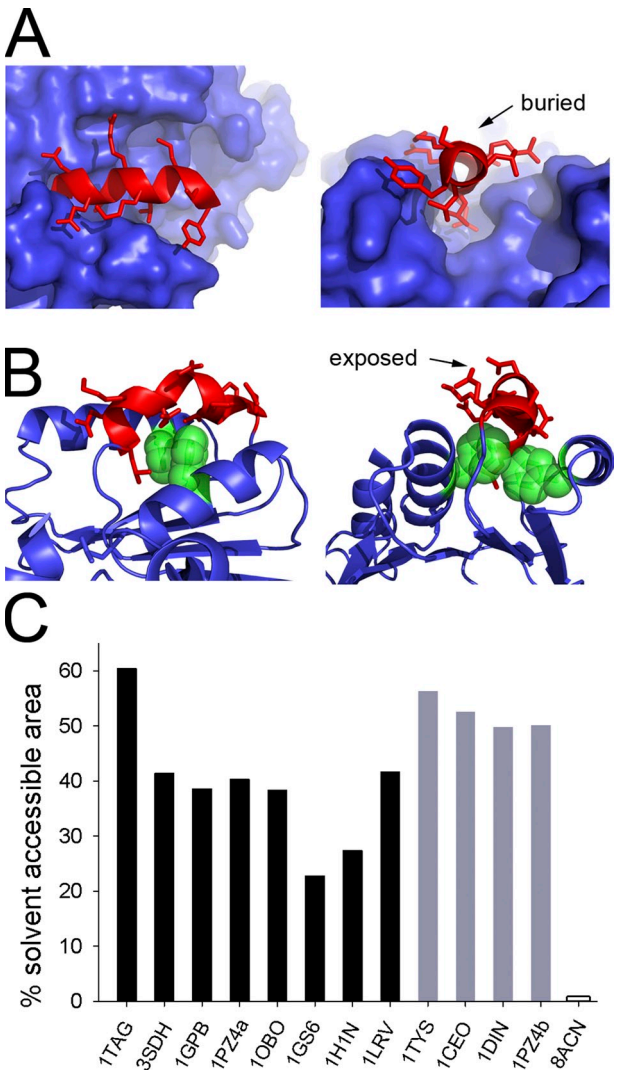

Figure 2. Packing modes of 3_{10} helices. (A) Mode A. Two views of the packing of a 10-residue-long 3_{10} helix (in red) in glycogen phosphorylase (Protein Data Bank accession no. 1GPB). The rest of the protein is shown as blue surface. (B) Mode B. Two views of packing of a 10-residue-long 3_{10} helix (in red) in dienelactone hydrolase (Protein Data Bank accession no. 1DIN). Two phenylalanine residues, shown as green CPK spheres, interact with the face of the 3_{10} helix. Other protein regions are shown as a blue cartoon. (C) Bar graph showing percentage of solvent-accessible surface area for each of the 3_{10} helices identified. Black bars indicate helices in packing mode A. Protein Data Bank accession numbers and residue numbering of respective 3_{10} helices: 1TAG, 201–208; 3SDH, 44–51; 1GPB, 515–524; 1PZ4, 95–103; 1OBO, 1040–1047; 1GS6, 405–412; 1H1N, 180–186; 1LRV, 172–178 (1LRV is a leucine-repeat protein with a 3_{10} helix present in each repeat; we have only considered one repeat in our analysis). Gray bars indicate helices in packing mode B. Protein Data Bank accession numbers and residue numbering of respective 3_{10} helices: 1TYS, 134–140; 1CEO, 241–248; 1DIN, 150–158; 1PZ4, 104–110. Empty bar indicates the fully encased 3_{10} helix (8ACN, 168–174).

3_{10} helices in potassium channels

Long 3_{10} helices have been described in the crystal structures of three potassium channels: the bacterial cyclic nucleotide–regulated potassium channel (MlotiK1) (Clayton et al., 2008) and the human Kv1.2 (Long et al., 2005a,b)- and Kv2.1-chimeric (Long et al., 2007) voltage-gated potassium channels. All of these channels belong to the superfamily of six-TM helix tetrameric cation channels and share the same three-dimensional architecture (Fig. 3 A).

In the structures of the Kv1.2- and Kv2.1-chimeric voltage-gated channels, the fourth TM helix (S4) adopts a 3_{10}-helical conformation over 7 and 10 residues, respectively. In these channels, S4 is the voltage sensor, a functionally important region with a conserved sequence motif ($R_1xxR_2xxR_3xxR_4xxK_5xxR_6$), where every third residue is positively charged (usually R_1 to R_6 are arginines, and K_5 is a lysine), and x's are large hydrophobic residues. S4 together with three other TM helices, S1, S2, and S3, forms the voltage sensor domain (Fig. 3 A). It has been well established that R_1 to R_4 are the charges that sense the membrane electrical field (Aggarwal and MacKinnon, 1996; Seoh et al., 1996). In the Kv2.1-chimeric channel, solved at 2.4 Å, the 3_{10} conformation stretches from R_3 to R_6, and the side chains of all charged residues in this stretch are buried within the rest of the voltage sensor domain (Fig. 3 B), forming salt bridges with negatively charged residues from S2 and S3. Residues R_1, which happens to be a glutamine in this channel, and R_2 are in an α-helical region and are partially exposed to the surrounding environment, probably corresponding to the hydrophilic groups of the phospholipid bilayer. In the Kv1.2 channel structure (Fig. 3 C), a recent re-refinement establishes that the 3_{10} conformation extends from R_4 to R_6, with the positively charged side chains in this stretch buried within the rest of the voltage sensor domain and shielded from the lipidic environment (Chen et al., 2010). These structures confirm the early suggestions of the presence of a 3_{10} conformation in the S4 of voltage-gated channels (Noda et al., 1984).

As a result of the voltage-gate channel structures, a role for the 3_{10}-helical conformation in voltage sensing has been proposed (Long et al., 2007; Clayton et al., 2008). It is widely accepted that the voltage-sensing mechanism involves translation of S4 across some part of the membrane; most likely, this translational movement is accompanied by a rotation, and some have suggested that S4 rotates along its axis (Tombola et al., 2006; Swartz, 2008). The details and extension of these movements are still a matter of discussion, but the 3_{10}-helical conformation offers an apparently simple explanation for some of the issues raised by the properties of S4.

Among these issues are: (a) the energetic cost of having positively charged residues translating through the low dielectric constant environment of the membrane, (b) the mechanistic basis behind the highly conserved sequence in S4, and (c) the mechanism of rotation of S4. First, the presence of the 3_{10} helix places many of the positively charged side chains at every third position on the same face, buried within the voltage sensor domain and shielded from the lipid environment. Therefore, the 3_{10} conformation solves issues (a) and (b) because if S4 were to adopt a totally α-helical conformation, some of the positively charged residues would necessarily be on the lipid apolar regions. Second, the conversion between the 3_{10}- and α-helical conformations observed in peptides, and described above, effectively results in a rotation of residues, and it provides a mechanistic model for issue (c). It has therefore been proposed that the transition between the 3_{10}- and α-helical conformations occurs during voltage sensing and that it is this movement that shields the positively charged residues away from the lipidic environment. It is possible that as shown in peptides, the conversion (rotation) is restricted to a fraction of the TM helix.

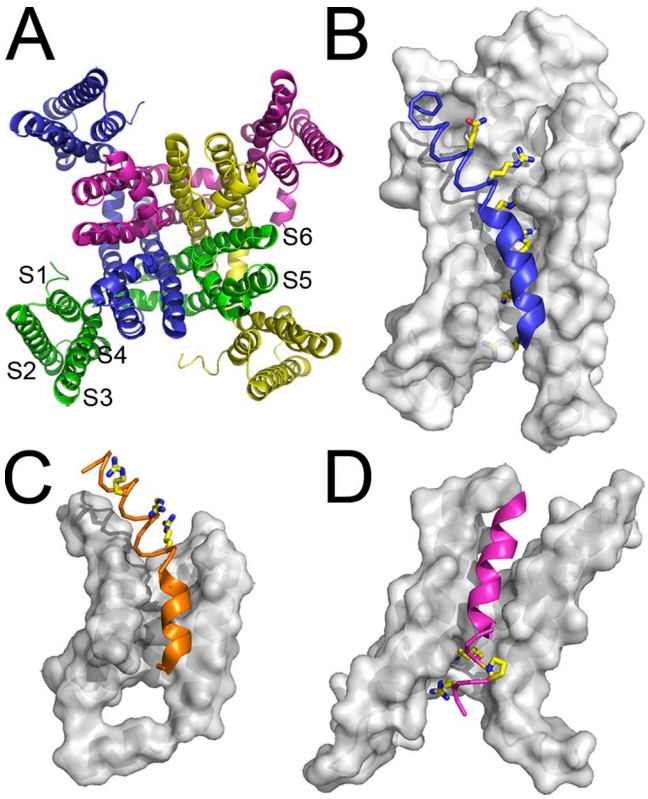

Figure 3. Domain architecture of six-TM channels. (A) Extracellular view of MlotiK1 structure, a bacterial cyclic nucleotide–regulated potassium channel, representative of the superfamily of six-TM helix cation channels. Subunits are shown in different colors. S1 to S4 compose the S1–S4 domain (structurally equivalent to a voltage sensor domain), and S5 and S6 (a pair from each subunit) form the pore domain. The voltage sensor domains of (B) Kv2.1-chimeric voltage-gated potassium channel and of (C) Kv1.2 voltage-gated potassium channel are shown in more detail. (D) The S1–S4 domain of the MlotiK1 channel. Surface representations correspond to S1, S2, and S3. Helices S4 are shown as a thin helical trace along α-helical segments and as a thick ribbon along 3_{10} stretches. Conserved positively charged residues, as well as MlotiK1 proline-108, are shown in stick model. The domains are oriented with the extracellular regions at the top of figure and cytoplasmic regions at the bottom. The N termini of S4 are on the extracellular side of the domains.

Several functional studies have recently explored or included the 3_{10} conformation of S4 as a component of voltage sensing. Villalba-Galea et al. (2008) have modeled the functional behavior of S4 in voltage sensor domains with three different states, resting, activated, and relaxed, in which transition from resting or activated to the relaxed state corresponded to a conversion between a 3_{10} and an α helix. In a voltage-gated sodium channel, cysteine cross-linking experiments between residues in S4 and residues in other helices of the voltage sensor have been interpreted with a model that includes the 3_{10} conformation (DeCaen et al., 2009). A recent report (Xu et al., 2010) of a minimal voltage sensor reinforces the functional importance of the S4 sequence periodicity (RxxR) and its implications for maintaining the 3_{10} conformation. Computational studies of voltage-gated channels have observed conversion of S4 between α- and 3_{10}-helical conformations, either during simulation of a channel in the resting state (Khalili-Araghi et al., 2010) or during simulation of the effects of membrane hyperpolarization in an activated-state channel (Bjelkmar et al., 2009).

In many of the studies considering the 3_{10} conformation as a component of voltage sensing, it has been proposed that shielding of the positively charged residues away from the apolar regions of the lipid/detergent phase is the major factor in the stabilization of the long 3_{10} helices. However, two other structures, those of the MlotiK1 channel (Clayton et al., 2008) and of the voltage sensor domain of the KvAP channel (Jiang et al., 2003), strongly suggest that the groove formed by S1, S2, and S3 also plays a role in the stability of the 3_{10} conformation.

MlotiK1 is a ligand-gated channel (Fig. 3 A) where opening and closing of the pore is induced by the binding of cyclic nucleotides to a C-terminal cytoplasmic domain (Clayton et al., 2004; Nimigean et al., 2004). In MlotiK1, S4 lacks the crucial R1, R2, R3, and R4 and is thought not to function as a voltage sensor. Importantly, S4 adopts a 3_{10}-helical conformation over a stretch of 11 amino acids, none of which are positively charged residues (Fig. 3 D). This observation demonstrates that the shielding of charged residues is not the only factor that stabilizes the 3_{10} conformation. Comparison of the structure of the voltage sensor domain from the Kv2.1-chimeric channel with the structure of the S1–S4 domain from MlotiK1 offers some clues about the stabilization of the 3_{10} helix in these channels. In these domains, S1, S2, and S3 form a groove where S4 fits (Fig. 3, B–D).

In MlotiK1, the whole length of S4 lies in a fairly straight groove and the 3_{10} becomes an α helix just before proline-108 in the helix, which ruptures the main-chain hydrogen-bonding network and appears to distort the helix (Fig. 3 D). In contrast, in the Kv2.1-chimeric channel the groove is not as extensive, disappearing on the extracellular half of the TM domain (Figs. 4 A and 3 B). Transition from the 3_{10}- to the α-helical conformation occurs around the region where the groove disappears and S4 is no longer tightly packed within the rest of the domain. In both channels, the 3_{10} helix coincides with the regions in S4 that are embedded within the groove formed by the other helices, just like in one of the 3_{10}-packing modes described above.

The structure of the voltage sensor domain from the bacterial voltage-gated KvAP channel also provides clues about stabilization of 3_{10} helices in these channels. This structure comprises the helices S1–S4 crystallized in complex with a monoclonal antibody; the channel's pore domain is missing (Jiang et al., 2003). S4 has a partial voltage sensor sequence that includes the crucial first four positively charged residues with canonical spacing (R1xxR2xxR3xxR4xx). Interestingly, this S4 does not adopt a 3_{10} conformation; it is all α helical. Superposition with the voltage sensor domain from the Kv2.1-chimeric channel reveals a very high degree of structural similarity (Fig. 4 B); however, the groove formed by S1, S2, and S3 in KvAP is much wider and shallower, and the α-helical S4 is no longer enveloped by the other helices in the domain. It is easy to conceive that S4 also adopts a 3_{10} conformation in the native KvAP channel. It is possible that truncation of the voltage sensor domain and/or binding of the antibody may have caused a rearrangement of the structure, leading to a change in the packing of S4 and the unwinding of its 3_{10} conformation. Regardless of what happens in the native KvAP structure, the comparison between the KvAP, MlotiK1, and Kv2.1-chimeric structures leads back to the idea we raised above, that the 3_{10} conformation has specific packing arrangements for its long-range stability (Fig. 4 C). In the structures of the voltage sensor/S1–S4 domains, the long helices packed in an almost parallel fashion create a groove that appears to be important for the stabilization of the 3_{10} conformation in S4.

3_{10} helices in membrane proteins

The observation of long 3_{10} helices in three potassium channels raises the possibility that other membrane proteins also have long 3_{10} helices. We analyzed ~233 structures of α-helical TM proteins that are deposited in the Protein Data Bank and catalogued in database maintained by the laboratory of Stephen White (White, 2004). To avoid low quality structures and structures of the same protein in different states, we reduced this already relatively small universe to a group of structures with nonredundant sequences at 3.2-Å resolution or better. Making use of the secondary structure analysis, which is associated with each coordinate file in the Protein Data Bank, we selected only the structures that contain 3_{10} helices with five residues or more and that have these 3_{10} helices positioned within their membrane-associated region, that is, either buried within the bilayer or positioned very close to the

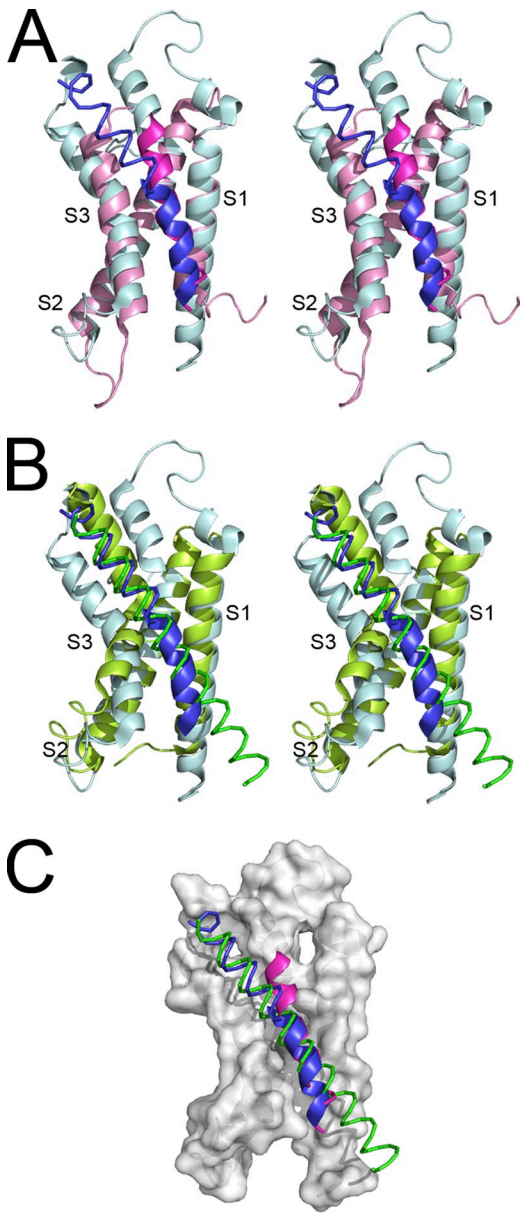

Figure 4. Superposition of voltage sensor and S1–S4 domains. (A) Stereoscopic view of a superposed voltage sensor domain from the Kv2.1-chimeric channel (blue) with the S1–S4 domain from the MlotiK1 channel (magenta). (B) Stereoscopic view of superposed voltage sensor domains from the Kv2.1-chimeric channel (blue) and from the KvAP channel (green). Domains were manually superposed by overlapping S1 and S2 from the different structures. (C) Comparison between the S4 of all three channels using the color code defined in A and B. α-Helical segments are shown as a thin helical trace, and 3_{10} sections are shown as a thick ribbon. Surface representation corresponds to S1, S2, and S3 from the Kv2.1-chimeric channel.

membrane surface. We found 25 structures for a total of 31 helices. Among these, we found 19 helices that are 5 residues long, 3 helices with 6 residues, 3 helices with 7 residues, and 3 helices with 8 residues; we also found 1 helix for each of following lengths: 9, 10, and 11 residues. The final group included the MlotiK1 and the Kv2.1-chimeric channels but not the Kv1.2 channel because of its close sequence relationship with the Kv2.1-chimeric channel. To compare our results with the previous analysis performed on soluble proteins (Enkhbayar et al., 2006), we calculated the frequency of helices for each length within the universe of helices with five residues or more, and plotted the results in Fig. 5 A. Within the clear limitations of our analysis, it is striking that for membrane proteins, 40% of the 3_{10} helices identified were longer than five residues, whereas in soluble proteins, this number was significantly smaller, just 20%. The higher frequency of long 3_{10} helices in membrane proteins is also clear when looking at defined helix lengths with seven or more residues. More structures are needed, but these results suggest that long 3_{10} helices are more prevalent in membrane proteins relative to soluble proteins. Strikingly, visual inspection of the 3_{10} helices in some of these membrane proteins reveals several interesting situations (Fig. 5, B–D): in cytochrome bc(1) complex (Protein Data Bank accession no. 2FYU), a 3_{10} helix with eight residues lies in a groove formed by the other TMs and is in close proximity to a heme, although not in direct contact with it; in the bacterial nitrate reductase A (Protein Data Bank accession no. 1Q16), a seven-residue-long 3_{10} helix directly coordinates the metal ion of a heme through a histidine side chain. The helix is packed between the heme and a phosphatidyl glycerol molecule; in the cyanobacterial photosystem II complex (Protein Data Bank accession no. 3BZ1), an eight-residue-long 3_{10} helix lies on top of a layer formed solely by lipids, chlorophyll A, and β carotene molecules, where it fits within a groove.

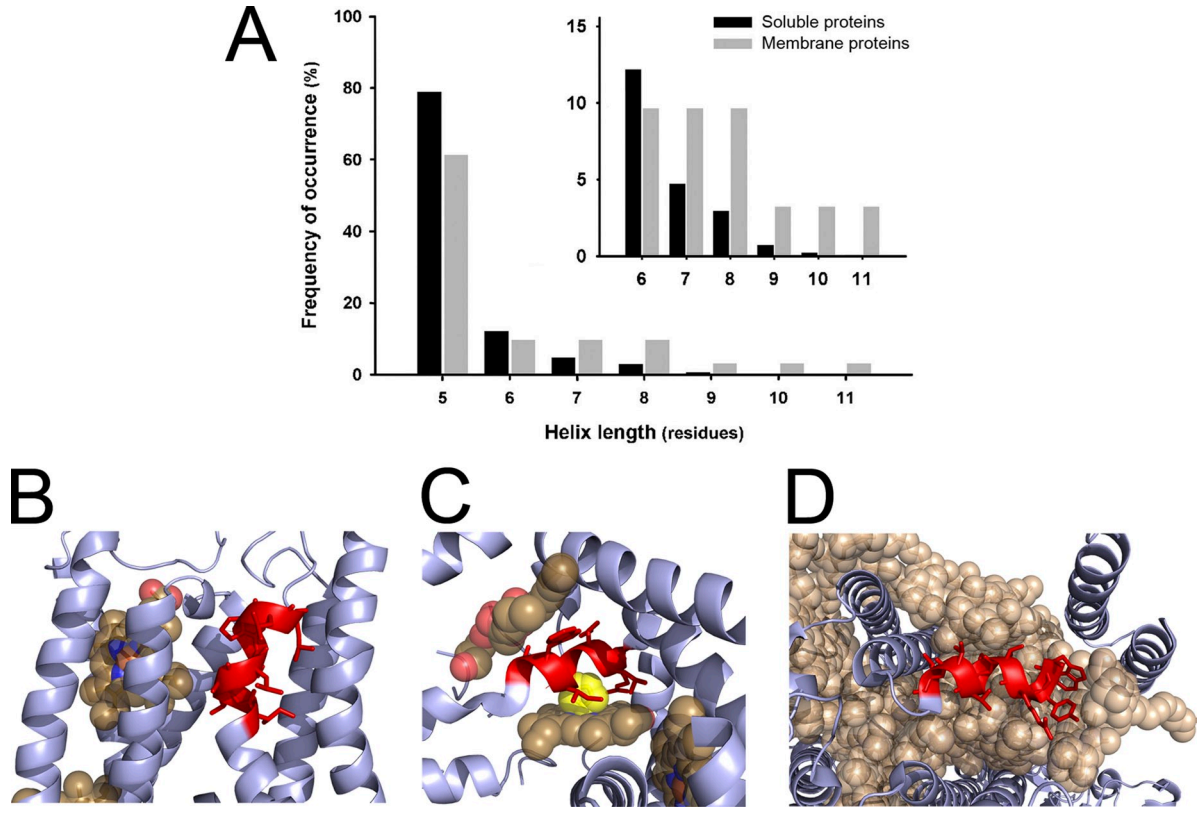

Figure 5. 3_{10} helices in other membrane proteins. (A) Graph comparing the frequency of 3_{10} helices in soluble and in membrane proteins. Only 3_{10} helices with lengths between 5 and 11 residues have been considered. The number of helices in each length category was normalized to the total number of detected helices with five or more residues. Inset shows in more detail the differences between membrane and soluble proteins for helices longer than six residues. The data for 3_{10} helices from soluble proteins has been extracted from Enkhbayar et al. (2006). Examples of 3_{10} helices in membrane proteins: 3_{10} helices are shown in red, other protein regions are shown as a blue ribbon, and prosthetic groups are shown as CPK spheres, unless otherwise indicated. (B) 3_{10} helix in cytochrome bc1 complex (Protein Data Bank accession no. 1FYU). Protoporphyrin IX containing Fe (heme) is shown in close proximity to the helix. (C) In bacterial nitrate reductase A (Protein Data Bank accession no. 1Q16), the iron atom from the heme is coordinated by histidine (yellow CPK spheres) from the 3_{10} helix. Opposite the heme and on the top side of the figure, there is phosphatidyl glycerol molecule completing the packing of the 3_{10} helix. (D) In the cyanobacterial photosystem II complex (Protein Data Bank accession no. 3BZ1), a 3_{10} helix is found embedded in a layer formed by LMG (1,2-distearoyl-monogalactosyl-diglyceride), β carotene, and chlorophyll A.

All of these examples raise interesting questions about the role of 3_{10} helices in these proteins: Do 3_{10} helices play structural and/or functional roles in these proteins? Do different protein functional states correspond to an interconversion between a 3_{10}- and α-helical conformation?

In conclusion, the structural and functional properties of long 3_{10} helices in proteins are still largely unexplored. For example, the sequence and structural context of these helices still need to be carefully analyzed. Further, the examples of long 3_{10} helices in membrane proteins and in particular in channels reveal potential functional roles that are just being unveiled and that will be the catalyst for many interesting experiments.

We thank Carol Harley and Artur Rodrigues for advice and comments.

Support for this work has been provided by European Molecular Biology Organization (installation grant), Fundação para a Ciência ea Tecnologia (FCOMP-010124-FEDER-007427/PTDC/QUI/66171/2006), and Marie-Curie Actions (IRG-239251).

Christopher Miller served as editor.

Submitted: 30 July 2010
Accepted: 12 November 2010

REFERENCES

Aggarwal, S.K., and R. MacKinnon. 1996. Contribution of the S4 segment to gating charge in the Shaker K+ channel. *Neuron*. 16:1169–1177. doi:10.1016/S0896-6273(00)80143-9

Armen, R., D.O. Alonso, and V. Daggett. 2003. The role of alpha-, 3(10)-, and pi-helix in helix—>coil transitions. *Protein Sci.* 12:1145–1157. doi:10.1110/ps.0240103

Barlow, D.J., and J.M. Thornton. 1988. Helix geometry in proteins. *J. Mol. Biol.* 201:601–619. doi:10.1016/0022-2836(88)90641-9

Bellanda, M., S. Mammi, S. Geremia, N. Demitri, L. Randaccio, Q.B. Broxterman, B. Kaptein, P. Pengo, L. Pasquato, and P. Scrimin. 2007. Solvent polarity controls the helical conformation of short peptides rich in Calpha-tetrasubstituted amino acids. *Chemistry (Easton)*. 13:407–416.

Bjelkmar, P., P.S. Niemelä, I. Vattulainen, and E. Lindahl. 2009. Conformational changes and slow dynamics through microsecond polarized atomistic molecular simulation of an integral Kv1.2 ion channel. *PLOS Comput. Biol.* 5:e1000289. doi:10.1371/journal.pcbi.1000289

Bowie, J.U. 1997. Helix packing angle preferences. *Nat. Struct. Biol.* 4:915–917. doi:10.1038/nsb1197-915

Chen, X., Q. Wang, F. Ni, and J. Ma. 2010. Structure of the full-length Shaker potassium channel Kv1.2 by normal-mode-based X-ray crystallographic refinement. *Proc. Natl. Acad. Sci. USA*. 107:11352–11357. doi:10.1073/pnas.1000142107

Chipot, C., and A. Pohorille. 1998. Folding and translocation of the undecamer of poly-L-leucine across the water-hexane interface. A molecular dynamics study. *J. Am. Chem. Soc.* 120:11912–11924. doi:10.1021/ja980010o

Clayton, G.M., W.R. Silverman, L. Heginbotham, and J.H. Morais-Cabral. 2004. Structural basis of ligand activation in a cyclic nucleotide regulated potassium channel. *Cell.* 119:615–627. doi:10.1016/j.cell.2004.10.030

Clayton, G.M., S. Altieri, L. Heginbotham, V.M. Unger, and J.H. Morais-Cabral. 2008. Structure of the transmembrane regions of a bacterial cyclic nucleotide-regulated channel. *Proc. Natl. Acad. Sci. USA*. 105:1511–1515. doi:10.1073/pnas.0711533105

Crisma, M., F. Formaggio, A. Moretto, and C. Toniolo. 2006. Peptide helices based on alpha-amino acids. *Biopolymers*. 84:3–12. doi:10.1002/bip.20357

DeCaen, P.G., V. Yarov-Yarovoy, E.M. Sharp, T. Scheuer, and W.A. Catterall. 2009. Sequential formation of ion pairs during activation of a sodium channel voltage sensor. *Proc. Natl. Acad. Sci. USA*. 106:22498–22503. doi:10.1073/pnas.0912307106

Dike, A., and S.M. Cowsik. 2006. Solution structure of amphibian tachykinin Uperolein bound to DPC micelles. *J. Struct. Biol.* 156:442–452. doi:10.1016/j.jsb.2006.07.006

Enkhbayar, P., K. Hikichi, M. Osaki, R.H. Kretsinger, and N. Matsushima. 2006. 3(10)-helices in proteins are parahelices. *Proteins*. 64:691–699. doi:10.1002/prot.21026

Fiori, W.R., K.M. Lundberg, and G.L. Millhauser. 1994. A single carboxy-terminal arginine determines the amino-terminal helix conformation of an alanine-based peptide. *Nat. Struct. Biol.* 1:374–377. doi:10.1038/nsb0694-374

Jiang, Y., A. Lee, J. Chen, V. Ruta, M. Cadene, B.T. Chait, and R. MacKinnon. 2003. X-ray structure of a voltage-dependent K+ channel. *Nature*. 423:33–41. doi:10.1038/nature01580

Karle, I.L., and P. Balaram. 1990. Structural characteristics of alpha-helical peptide molecules containing Aib residues. *Biochemistry*. 29:6747–6756. doi:10.1021/bi00481a001

Karle, I.L., J.L. Flippen-Anderson, R. Gurunath, and P. Balaram. 1994. Facile transition between 3(10)- and alpha-helix: structures of 8-, 9-, and 10-residue peptides containing the -(Leu-Aib-Ala)2-Phe-Aib-fragment. *Protein Sci.* 3:1547–1555. doi:10.1002/pro.5560030920

Khalili-Araghi, F., V. Jogini, V. Yarov-Yarovoy, E. Tajkhorshid, B. Roux, and K. Schulten. 2010. Calculation of the gating charge for the Kv1.2 voltage-activated potassium channel. *Biophys. J.* 98:2189–2198. doi:10.1016/j.bpj.2010.02.056

Long, S.B., E.B. Campbell, and R. Mackinnon. 2005a. Crystal structure of a mammalian voltage-dependent Shaker family K+ channel. *Science*. 309:897–903. doi:10.1126/science.1116269

Long, S.B., E.B. Campbell, and R. Mackinnon. 2005b. Voltage sensor of Kv1.2: structural basis of electromechanical coupling. *Science*. 309:903–908. doi:10.1126/science.1116270

Long, S.B., X. Tao, E.B. Campbell, and R. MacKinnon. 2007. Atomic structure of a voltage-dependent K+ channel in a lipid membrane-like environment. *Nature*. 450:376–382. doi:10.1038/nature06265

Mikhonin, A.V., and S.A. Asher. 2006. Direct UV Raman monitoring of 3(10)-helix and pi-bulge premelting during alpha-helix unfolding. *J. Am. Chem. Soc.* 128:13789–13795. doi:10.1021/ja062269+

Nimigean, C.M., T. Shane, and C. Miller. 2004. A cyclic nucleotide modulated prokaryotic K^+ channel. *J. Gen. Physiol.* 124:203–210. doi:10.1085/jgp.200409133

Noda, M., S. Shimizu, T. Tanabe, T. Takai, T. Kayano, T. Ikeda, H. Takahashi, H. Nakayama, Y. Kanaoka, N. Minamino, et al. 1984. Primary structure of Electrophorus electricus sodium channel deduced from cDNA sequence. *Nature*. 312:121–127. doi:10.1038/312121a0

Pal, L., and G. Basu. 1999. Novel protein structural motifs containing two-turn and longer 3(10)-helices. *Protein Eng.* 12:811–814. doi:10.1093/protein/12.10.811

Pauling, L., R.B. Corey, and H.R. Branson. 1951. The structure of proteins; two hydrogen-bonded helical configurations of the polypeptide chain. *Proc. Natl. Acad. Sci. USA*. 37:205–211. doi:10.1073/pnas.37.4.205

Peters, J.W., M.H. Stowell, and D.C. Rees. 1996. A leucine-rich repeat variant with a novel repetitive protein structural motif. *Nat. Struct. Biol.* 3:991–994. doi:10.1038/nsb1296-991

Raman, S.S., R. Vijayaraj, R. Parthasarathi, and V. Subramanian. 2008. Helix forming tendency of valine substituted poly-alanine:

a molecular dynamics investigation. *J. Phys. Chem. B.* 112:9100–9104. doi:10.1021/jp7119813

Seoh, S.A., D. Sigg, D.M. Papazian, and F. Bezanilla. 1996. Voltage-sensing residues in the S2 and S4 segments of the Shaker K+ channel. *Neuron.* 16:1159–1167. doi:10.1016/S0896-6273(00)80142-7

Swartz, K.J. 2008. Sensing voltage across lipid membranes. *Nature.* 456:891–897. doi:10.1038/nature07620

Tirado-Rives, J., and W.L. Jorgensen. 1991. Molecular dynamics simulations of the unfolding of an alpha-helical analogue of ribonuclease A S-peptide in water. *Biochemistry.* 30:3864–3871. doi:10.1021/bi00230a009

Tombola, F., M.M. Pathak, and E.Y. Isacoff. 2006. How does voltage open an ion channel? *Annu. Rev. Cell Dev. Biol.* 22:23–52. doi:10.1146/annurev.cellbio.21.020404.145837

Villalba-Galea, C.A., W. Sandtner, D.M. Starace, and F. Bezanilla. 2008. S4-based voltage sensors have three major conformations. *Proc. Natl. Acad. Sci. USA.* 105:17600–17607. doi:10.1073/pnas.0807387105

White, S.H. 2004. The progress of membrane protein structure determination. *Protein Sci.* 13:1948–1949.

Xu, Y., Y. Ramu, and Z. Lu. 2010. A shaker K+ channel with a miniature engineered voltage sensor. *Cell.* 142:580–589. doi:10.1016/j.cell.2010.07.013